THE TEMPERATURE STRUCTURE IN A STABLY STRATIFIED INTERNAL BOUNDARY LAYER OVER A COLD SEA

DIMITRIOS MELAS

Department of Meteorology, University of Uppsala, Box 516, S-75120 Uppsala, Sweden

(Received 4 April, 1989)

Abstract. Data from the Öresund experiment are used to investigate the structure of the stably stratified internal boundary layer (SIBL) which develops when warm air is advected from a heated land surface over a cooler sea. The present study is based on a theory developed by Stull (1983a, b, c). He proposed that the turbulence and the mean structure of the nocturnal boundary layer is controlled by the time-integrated value of surface heat flux and that the instantaneous heat flux is of less importance.

Dimensional arguments are used to define simple, physically consistent, temperature, velocity and length scales. The dimensionless surface heat flux has a high value immediately downwind of the shoreline and it decreases rapidly in magnitude with increasing distance from the coast. Farther away, it is essentially constant. The dimensionless potential temperature change exhibits an exponential profile. It is estimated that turbulence accounts for 71% of boundary-layer cooling while clear-air radiational cooling is responsible for the remaining 29%.

Finally it is found that theoretical predictions for the height of the SIBL are in a good agreement with observations.

List of Symbols

c_p specific heat at constant pressure
f coriolis parameter
g acceleration due to gravity
h depth of the SIBL
H heat-flux-history length scale
k von Kàrmàn's constant
p air pressure reduced to mean sea level
Q_H surface sensible heat flux
$\bar{R}$ net radiative cooling for the whole SIBL integrated over distance from the shoreline
$\bar{S}_\theta$ potential temperature change due to the net radiative flux divergence
u_* friction velocity
u_g component of the geostrophic wind normal to the coastline
U_g geostrophic wind speed
$\bar{U}_r$ representative layer-averaged wind speed
V_s turbulence generation velocity scale $= (fU_g z_0)^{1/2}$
w vertical wind velocity
$\overline{w\theta}$ kinematic heat flux
x distance downwind from the shoreline
X dimensionless distance $= x(g\Delta\theta_s/\theta)/u^2$
x_c coordinate of a station given in UTM (universal transverse mercator) east
y_c coordinate of a station given in UTM north
z height above the earth's surface
z' $= z - 1.3$ m
z_0 aerodynamic roughness length
$\Delta\theta$ $= \theta_{sea}(x, z') - \theta_{Bb}(z')$

Boundary-Layer Meteorology **48**: 361–375, 1989.

$\Delta\theta_s$ $= \theta_{Bb}(1.3) - \theta_w$
$\Delta\theta'_s$ $= \theta_{sea}(1.3) - \theta_{Bb}(1.3)$
θ potential temperature
θ_{Bb} potential temperature of the air at the Barsebäck mast
θ_{sea} potential temperature of the air over the sea
θ_w potential temperature of the water surface
θ_* temperature scale for the surface layer
ρ density of air
ϕ dimensionless gradients in the surface layer

1. Introduction

When warm air is advected from land out over a cooler sea, it is extensively modified by the underlying surface. As a result, a stably stratified internal boundary layer (SIBL) develops as a function of downwind distance. Contrary to the convective and neutral internal boundary layers which have been investigated rather thoroughly, there has been little effort to describe the flow from a warm to a cool surface. The first attempt to describe the growth of the SIBL was made by Mulhearn (1981), who based the analysis on dimensional arguments. The same approach was reproduced by Gryning and Joffre (1987) in studying the wind field modification using data from the Öresund experiment. Garratt (1987) was concerned with the same problem using a two-dimensional mesoscale numerical model. A common feature of these studies is that the horizontal scale ranges between some tens to several hundreds of kilometres. This is at least one order of magnitude larger than the horizontal scale of the convective IBL studies and reveals the slow growth rate of the SIBL.

The SIBL developing over a cooler surface is often exemplified as a steady-state stable boundary layer. On the other hand, the nocturnal boundary layer (NBL), which forms at night over land, is often treated as a horizontally homogeneous stable boundary layer. It is clear that the SIBL has many similarities with the NBL, the main difference being the relative importance of the advection terms and the time rate of change term in the potential temperature equation. The purpose of this paper is to show that a heat-flux history length scale proposed by Stull (1983a, b, c) for the NBL over land can also be used in analyzing the structure of the SIBL. The evolution of this modified layer will be described in terms of imposed external forcings such as pressure gradient force, surface roughness, and potential temperature difference between sea and land surface. The study is based on experimental data from the Öresund experiment (see Section 3).

2. Theory

According to Brost and Wyngaard (1978), the NBL adjusts very slowly to changing surface conditions and is typically not in equilibrium with its surface forcings. Caughey *et al.* (1979) estimated that the time required for the influence

of changed surface conditions to reach the upper levels of the NBL is typically about seven hours. Due to weak turbulence, changes in surface forcing are communicated only very slowly across the depth of the NBL. In spite of this, the effects of the changing surface conditions are accumulated within the NBL resulting in a (lagged) change in its structure.

With such a philosophy in mind, Stull (1983a) argued that the instantaneous heat flux may not be a governing parameter for the NBL temperature structure; he suggested instead that an accumulation-type length scale based on the night-time heat-flux history was relevant for the NBL. This length scale is defined as

$$H = \int_0^t (Q_H/\rho c_p)\,\mathrm{d}\tau/\Delta\theta_s\,, \tag{1}$$

where t is the time since the evening transition, Q_H is the surface sensible heat flux, ρ is the density of air, c_p is the specific heat of air at constant pressure, τ is a dummy of integration, and $\Delta\theta_s$ is a temperature scale equal to the surface potential temperature change. In a Lagrangian framework, the definition of this length scale is modified to yield

$$H(x) = \int_0^x (Q_H(x)/\rho c_p)\,\mathrm{d}x/(\bar{U}_r\Delta\theta_s)\,, \tag{2}$$

where x is the distance downwind from the surface change, and $\bar{U}_r$ is a representative layer-averaged wind speed.

The above definition of a heat-flux history length scale includes only the sensible heat flux and neglects contributions from other sources such as latent heat flux, clear-air radiation cooling and subsidence. Although the latent heat flux is a large part of the thermal energy transfer at the sea surface, latent heating of the boundary layer is negligible unless the air is saturated. On the other hand, the net radiative-flux divergence may contribute considerably to the development of the surface-based inversion layer and cannot be neglected. In the present study, radiational cooling is not included explicitly but it is estimated as a residual. Clearly, this is justified only when boundary-layer cooling is dominated by the turbulent heat flux divergence. In the SIBL, the turbulence heat flux is associated with horizontal advection which is, by far, the largest term in the heat budget of the boundary layer. Further evidence for not including radiational cooling in Equation (2) is presented in Section 5. Finally, subsidence brings down warmer air from aloft and also implies a slower growth rate of the boundary layer. Heating rates due to subsidence are sometimes comparable with turbulent cooling rates and cannot always be neglected (see, e.g., Carlson and Stull, 1986). Unfortunately, subsidence is very difficult to measure but it can be crudely estimated from radiosonde ascents. For the data set analysed in the present study,

we found vertical velocities of minus a few cm/s at 2000 m. Assuming the divergence to be constant with height, a crude estimate of the subsidence warming $(-w\partial\theta/\partial z)$ at 100 m is $\sim 5 \times 10^{-6}$ K/s which is at least one order of magnitude less than turbulent cooling.

3. The Data Set

The theory proposed by Stull (1983a) has been tested against data from the Öresund experiment which took place over the Öresund, the 20 km wide strait between Denmark and Sweden; see Gryning (1985) for a detailed account. This was an international experiment with participation from 15 institutions in the Nordic countries (Denmark, Finland, Norway and Sweden) and in Belgium, Germany and the Netherlands. The experimental campaign was carried out during the period May 15 to June 15, 1984 while a special intensive measuring program was carried out during the period 4–10 June. The meteorological observation network was designed to obtain information of the flow field along a 80-km long traverse across the Öresund.

The Öresund region is well suited for investigations of the inhomogeneous boundary layer, because the coastlines on both sides of the strait are rather straight and practically parallel, and the land area is fairly flat. During the experimental period, the sea surface temperature was usually lower than that of the land surface so a stably stratified internal boundary layer develops as air passed over the cold water surface.

(a) The measurements

The locations of the measurement sites used in the present study are shown in Figure 1. They have been chosen to represent the meteorological conditions over land upwind of the coastline and over the water surface.

During the intensive measuring period of the Öresund experiment, the research vessel Aranda moved between five positions in the Öresund (points A–E), making near-surface measurements of wind and temperature fields. The ship remained for one hour at each position and a total of 72 measurements were carried out during the experiment. The prevailing winds during this period were from the east and average one-hour upstream (overland) profiles were taken from a small mast (12 m) at Barsebäck beach (Bb). Simultaneous wind and temperature profiles measured at the western coast of Öresund, at the Charlottenlund site (Ch), were also used as representative of over sea conditions.

Table I shows the measurement heights at the different sites.

Additionally the temperature profiles measured by minisonde ascents over the water will be used to determine the height of the stable IBL.

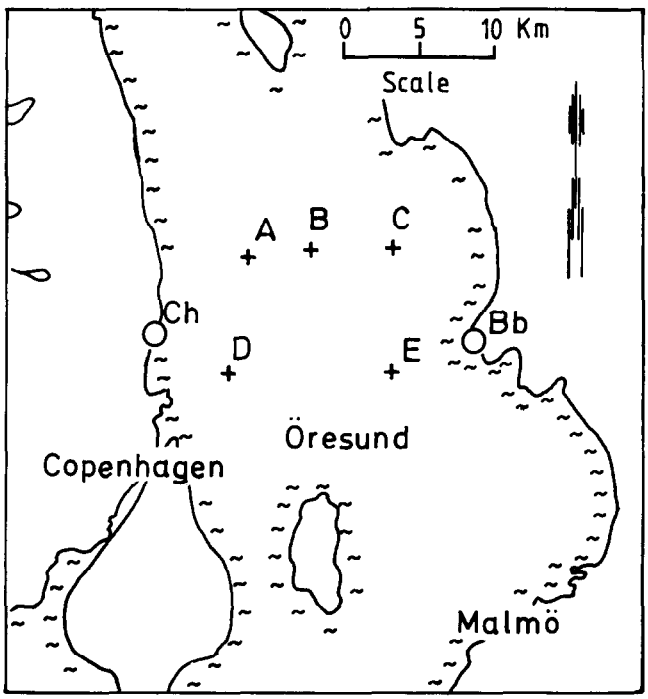

Fig. 1. Map of the Öresund area, showing the measurement sites: Bb and Ch are the locations of the Barsebäck and Charlottenlund masts respectively, and A, B, C, D and E are the five positions where the research vessel Aranda performed measurements.

(b) Derived quantities

Unfortunately, no turbulence measurements over the water are available. Thus, we had to estimate the momentum and heat fluxes through indirect techniques. Launiainen *et al.* (1987) used bulk transfer coefficients to derive the turbulent fluxes from the mean wind and temperature measured on the ship Aranda. At Barsebäck and Charlottenlund, the same quantities were derived using the flux-profile relationship method. The Monin–Obukhov (M–O) similarity theory is now well established and indirect techniques provide stable and representative estimates of the surface fluxes. However there still exists some controversy about

TABLE I

The measurement heights (SS is the sea surface)

	Wind speed	Temperature	Wind direction
Barsebäck	1.6, 3.5, 12.2 m	1.3, 3.1, 11.8 m	12.0 m
Aranda	8.2 m	SS, 10.8 m	10.8 m
Charlottenlund	6.0, 11.5 m	5.7, 11.2 m	12.8 m

the exact form of the dimensionless gradients, ϕ, and the value of von Kàrmàn's constant, k. In the present study we used the ϕ functions proposed by Högström (1988) together with $k = 0.40$. A far more delicate task is to solve the problems associated with the inhomogeneous terrain and inadequate profile measurements. The Aranda measured the wind velocity only at one height and the neutral drag coefficient for the water surface was obtained from other studies. Since the measurements were often taken near the Swedish coast, the limited fetch may lead to an error in the calculated flux. The Charlottenlund mast was erected about 18 m from the coastline and it is expected that the lowest levels are affected by the land surface. Thus it was decided to use only the measurements above the 5 m level. Finally, there were horizontal differences in the sea surface temperature and, as was shown by satellite images, there existed a narrow region (~0.5 km) of warm shallow water near the coastline on both sides of the Öresund. These "practical" problems are the main sources for the uncertainty in surface fluxes calculations.

The friction velocity u_* and the temperature scale θ_* were also used in the corresponding M–O expressions to interpolate the wind and the temperature to fixed levels. Finally geostrophic winds were calculated from an objective analysis of the reported pressures from 41 stations. The pressure field was described by fitting different polynomials to the measured pressures; in particular

$$p(x_c, y_c) = \sum_{s=0}^{n} \sum_{t=0}^{n} a_{st} x_c^s y_c^t , \tag{3}$$

where $p(x_c, y_c)$ is the pressure reduced to mean sea level and x_c, y_c are the coordinates of the stations. The coefficients a_{st} are determined by least squares. The main objective of the analysis method is to reduce the impact of instrumental and observational errors upon the analysed field and to determine the optimum polynomial order in Equation (3). Details of the analysis method are found in Hedegaard (1985) and Melas (1987).

4. Parameterization of the Length Scale H

Estimated values of u_* and θ_* are rather sparse, so we have to parameterize the variation of the heat-flux with distance from the coastline in order to calculate the heat-flux history length scale. We shall develop a formulation based on simple physical and dimensional arguments.

Gryning and Joffre (1987) showed that the modification of the wind speed as air passes over the Öresund can be explained fairly well using a dimensionless distance $X = x(g\Delta\theta_s/\theta)/u^2$. In the present study, we have used $\Delta\theta_s = \theta_{Bb}(1.3) - \theta_w$, where θ_{Bb} is the potential temperature at the Barsebäck mast and θ_w is the water temperature measured on the ship Aranda, and $u = u_g$, where u_g is the component of the geostrophic wind normal to the coastline.

We expect that the properly nondimensionalized heat flux will be a function of

the dimensionless distance, X. Two scales will be formulated using dimensional and physical arguments.

In the stably stratified boundary layer, turbulence is generated only mechanically and Stull (1983b) proposed a "turbulence generation" velocity scale $V_s = (fU_g z_0)^{1/2}$, which is related to the combined ability of pressure-gradient force (fU_g) and surface roughness (z_0) to generate turbulence. Here it is assumed that wind shear is created only at the ground by friction acting on the ambient flow. This is not always valid and it is anticipated that V_s will not be the appropriate scale when wind shear is generated by other processes (e.g., baroclinicity, low level jets, etc.).

The roughness length of the sea surface is not an external parameter of the flow. The sea is a fluid lower boundary and interacts dynamically with the air above. Thus, it is expected that the roughness length increases with wind speed. Over the oceans, Charnock's relation between the roughness length and the wind stress is well established but in a narrow strait like Öresund, this kind of approach may lead to an error due to limited fetch. Thus, for simplicity we have decided to use a constant value for the roughness length of the water surface, equal to 0.0001 m. This is roughly equal to the mean value of the roughness length estimated from the Aranda ship measurements.

We have already selected $\Delta\theta_s$ as the proper temperature scale. Melas (1987) analysed the pressure field during the 4th and the 5th June, the two most often modelled days in the Öresund data set, and found that, during the 5th of June, calculated surface geostrophic winds are considerably lower than the winds measured at 2000 m by radiosonde ascents. This was attributed to baroclinicity and isalobaric winds. The stably stratified IBL is rather shallow and the effects of the baroclinicity are probably of less significance, but the rapidly changing pressure field upset the geostrophic equilibrium. Thus it was decided to exclude from our data set the periods during which calculated geostrophic winds were much lower than the observed ones at 2000 m. In what follows, $u_*\theta_* = \overline{w\theta}$, the kinematic heat flux, is simply called the heat flux, a convention often used in the literature.

The ranges of the parameters included in the present study are as follows,

Fetch, x:	6000–30 000 m
Surface temp. change, $\Delta\theta_s$:	0.3–9.8 K
Geostrophic wind speed, U_g:	6.9–19.0 m/s
Geostrophic wind direction, WD_g:	57°–154°
Heat flux, $u_*\theta_*$:	0.0017–0.0554 K m/s

Figure 2 shows the dimensionless heat flux, $u_*\theta_*/(V_s\Delta\theta_s)$, as a function of the dimensionless distance, X. A second-order logarithmic curve has been fitted to the data:

$$-u_*\theta_*/(V_s\Delta\theta_s) = -27.3 + 8.7\ln(X+1) - 0.9\ln^2(X+1)\,. \qquad (4)$$

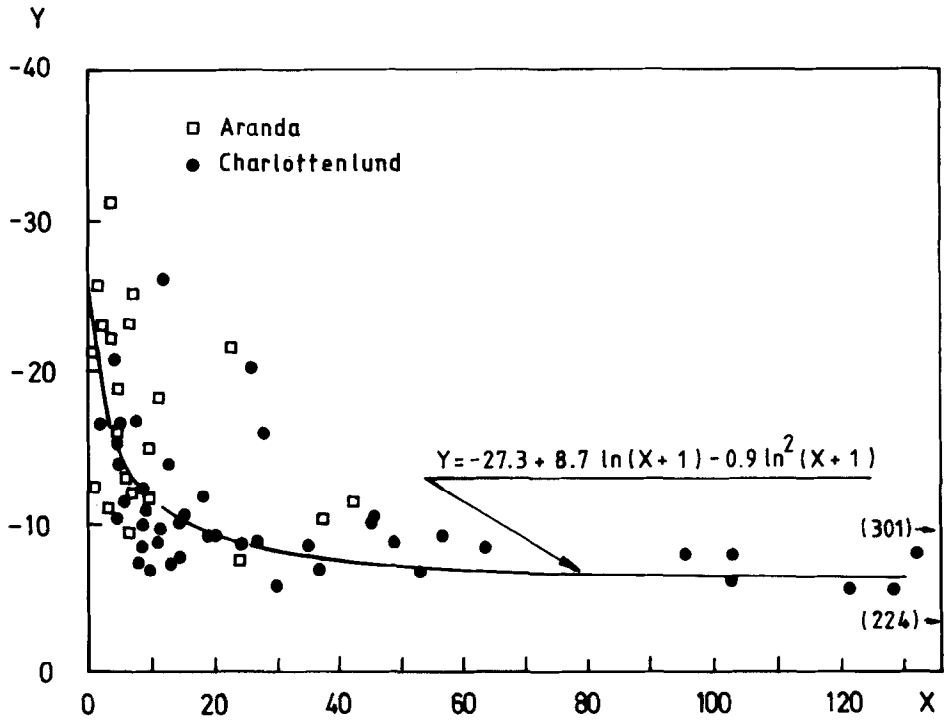

Fig. 2. The dimensionless heat flux, $Y = -u_* \theta_* / (V_s \Delta\theta_s)$, plotted as a function of the dimensionless overwater fetch $X = g(x\,\Delta\theta_s/\theta)/u_g^2$.

The dimensionless heat flux shows a high value immediately downwind of the coastline, although the exact value of the intercept in Equation (4) is rather uncertain because of the sharp gradient of the heat flux in a narrow region near the coastline. This high value is not surprising, considering that the temperature difference between the advected warm air and the underlying sea surface is also high immediately downwind of the surface change. The sharp gradient of the heat flux in the region near the coastline can be attributed to decaying turbulence advected from the land. This is very effective in mixing some of the cooler air upward and therefore in reducing the temperature gradient. Farther downwind, static stability suppresses the turbulence and the adjustment process becomes very slow. In this region, the heat flux is essentially constant. Launiainen *et al.* (1987), when analyzing the Aranda data set, found rather small horizontal differences in the sensible heat flux. The accumulated turbulent cooling within the SIBL can be determined by integrating Equation (4).

In order to calculate the length scale H (Equation 2), we must first determine $\bar{U}_r$, the representative layer-averaged wind speed. This is not a trivial task, as the wind velocity at any height inside the stably stratified IBL shows a strong variation with distance from the coastline (see e.g., Doran and Gryning, 1987 and

Gryning and Joffre, 1987). In addition, the representative layer-averaged wind speed depends on the SIBL height, which in turn is a function of fetch. These two effects partly cancel each other, and since we could not find a straightforward method to account for them, we have used the observed wind speed at 10 m height as a representative wind speed. This is not valid for very short fetches where the SIBL is still very shallow.

The representative layer-average wind speed is not an external parameter of the flow but, as Gryning and Joffre (1987) show, the modification of the wind speed at 10 m height can be described by the following relationship:

$$u_{\text{sea}}(10)/u_{\text{land}}(10) = 1.75 - 0.2\ln(X) \tag{5}$$

where X is the dimensionless distance. Knowing the wind speed over the land, the representative layer-average wind speed can be calculated from Equation (5).

5. The Potential Temperature Change Profile

The evolution of the temperature in a stably stratified boundary layer is governed by four transport processes: horizontal advection, subsidence, turbulence, and radiation. The relative contribution of each of these processes is of vital importance for the potential temperature profile. Thus, the wide variety of the proposed potential temperature profile shapes is not surprising (see e.g., Stull, 1988 for a summary). It is evident that a unique shape does not exist but it depends upon the forcings acting on the boundary layer. The present study treats only the potential temperature change when air encounters the cooler water surface and is not concerned with the potential temperature profile itself. During typical daytime conditions, the boundary layer over the land is in an unstable state and the potential air temperature is nearly constant throughout the boudary layer except in the layer near the ground. In this case, the shapes of the potential temperature change profile and the potential temperature profile inside the SIBL match.

Stull (1983a) proposed that the dimensionless potential temperature change, $\Delta\theta/\Delta\theta'_s$, is a function only of the dimensionless height, z'/H. The potential temperature change at any height is defined as $\Delta\theta = \theta_{\text{sea}}(x, z') - \theta_{\text{Bb}}(z')$ and the surface potential temperature change as $\Delta\theta'_s = \theta_{\text{sea}}(1.3) - \theta_{\text{Bb}}(1.3)$. It was necessary to change slightly the definition of the temperature scale used in the parameterization of H (Equation 4) so that $\Delta\theta/\Delta\theta'_s$ approaches unity when z'/H approaches zero. Consequently we define $z' = z - 1.3$ m.

In order to isolate the advection effects on the temperature structure, we shall neglect the temperature change with time. This is mainly justified during daytime conditions when the temperature difference between the land and the water surface is large. The following analysis is restricted only to these cases when $\Delta\theta'_s > 1$ K.

Figure 3 shows the dimensionless potential temperature change plotted against

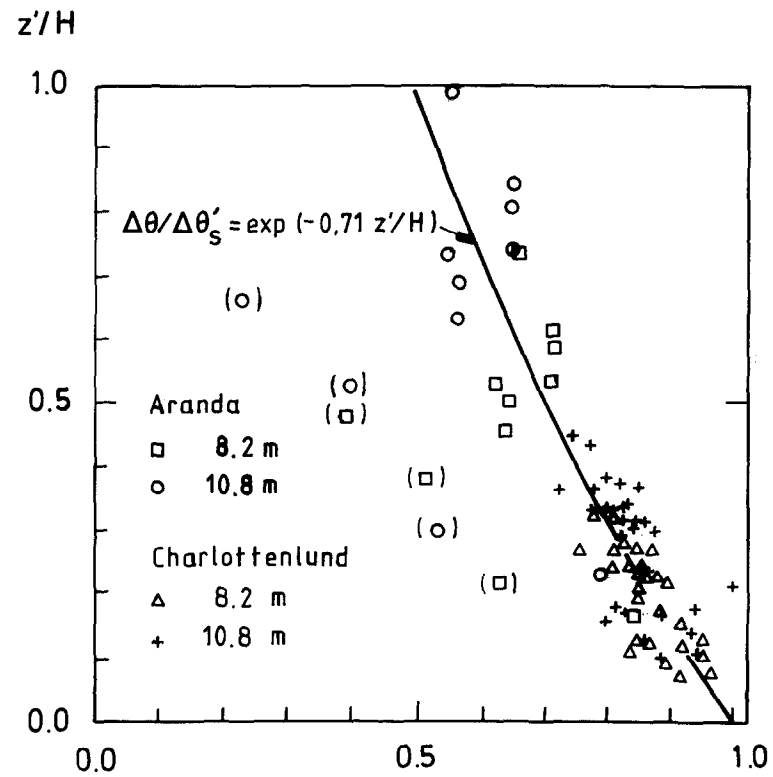

Fig. 3. The dimensionless potential temperature change, $\Delta\theta/\Delta\theta'_s$, plotted against the dimensionless height, z'/H. Symbols in parenthesis represent transitional conditions.

dimensionless height. An exponential curve provides a good eye-fit to the data:

$$\Delta\theta/\Delta\theta'_s = \exp(-0.71 z'/H) . \tag{6}$$

The six data points within parenthesis correspond to three temperature profiles measured during transition periods.

The coefficient $a = 0.71$ in Equation (6) is surprisingly near the value 0.77 found by Stull (1983a) using Wangara and Koorin boundary-layer data.

The exponential profile shape implies a negative curvature for the temperature profiles. André and Mahrt (1982) discussed the relative contributions of radiative and turbulent cooling to the development of the nocturnal surface inversion and suggested that strong negative profile curvature is associated with a dominance of radiative cooling. Neglecting subsidence and the time change of temperature, the potential temperature equation for the two-dimensional case is,

$$\bar{U}\,\partial\bar{\theta}/\partial x = -\partial\overline{w\theta}/\partial z + \bar{S}_\theta , \tag{7}$$

where $\bar{S}_\theta$ is the potential temperature change due to net radiative flux divergence. Equation (7) can be integrated over distance (from the shoreline) and over height (from the surface to some fixed height well above the SIBL height) to yield

$$H\,\Delta\theta s\bar{U}_r/0.71 = H\,\Delta\theta s\bar{U}_r + \bar{R} \tag{8}$$

where $\bar{R}$ is the net radiative cooling for the whole SIBL integrated over distance from the shoreline. In order to obtain Equation (8), we made the following assumptions:

(1) The potential temperature change is expressed by Equation (6).
(2) Cooling above the SIBL is negligible. This is an often quoted definition for the internal boundary layer. Unfortunately, clear-air radiational cooling and subsidence make this definition sometimes rather shaky. For the purpose of these calculations it is satisfactory to state that the uncertainty introduced by this assumption is rather small. This is apparently true, because turbulence associated with advection dominates the growth of the SIBL. Although the relative importance of radiational cooling and subsidence is expected to increase with height above the surface, their significance is restricted by the shallowness of the SIBL.
(3) $\bar{U}$ in Equation (7) is replaced by $\bar{U}_r$, the representative layer-averaged wind speed.

From Equation (2) we realize that $H\,\Delta\theta s\bar{U}_r$ is the accumulated cooling of the SIBL due to turbulence transport, and we may estimate that the radiational cooling is about 41% of the turbulent cooling. Consequently, 29% of the total cooling inside the SIBL is due to clear-air radiational cooling and 71% is due to turbulent transport. This indicates that the negative curvature of the temperature profiles in this case is not related to the relative magnitude of radiative cooling but is rather due to advection effects.

6. Depth of the Stable IBL

Usually the depth of the stably stratified boundary layer is defined either as the depth of the surface inversion or as the depth of the turbulent layer adjacent to the ground. Since the upper part of the inversion layer is usually non-turbulent, these different definitions often provide different estimates for the depth of the stable boundary layer. Unfortunately, there is also a wide variety of definitions for the depth of the surface inversion and the turbulent layer. Measurements reveal also that the top of the stable boundary layer is not always sharply demarked.

Stull (1983a) defined the top of the NBL as that height where the potential temperature change is 2% of the surface value. Then the exponential profile (Equation 6) implies that the height of the SIBL, h, is expressed by

$$h = 5.5H\,. \tag{9}$$

Unfortunately, there are only a few minisonde ascents over the Öresund which can be used to estimate h. In all cases but one, the transition between the surface inversion and the slightly stratified layer above is rather sharp, and the top of the SIBL can be estimated with fair accuracy.

Figure 4 shows one of the minisonde profiles. The potential temperature profile reveals a strong inversion layer near the water surface and a weak elevated inversion above 74 m. This elevated inversion is due to large-scale subsidence, which does not affect our results considerably. The parameterized SIBL depth, $h = 75$ m, provides a very good estimate for the depth of the surface-based inversion layer. It is noticed that the minisonde was launched at a position about 12 km from the Swedish coast. This indicates that the stably stratified IBL grows very slowly with an average fetch-to-height ratio of about 160. This can be compared with the results of Raynor *et al.* (1979) who found, for the unstable IBL over land, an average fetch-to-height ratio of about 30.

Table II shows a comparison between the observed and the parameterized height of the SIBL. Good agreement is achieved in almost all cases. On the 5th of June, the predicted SIBL height is lower than the observed one, but there is an

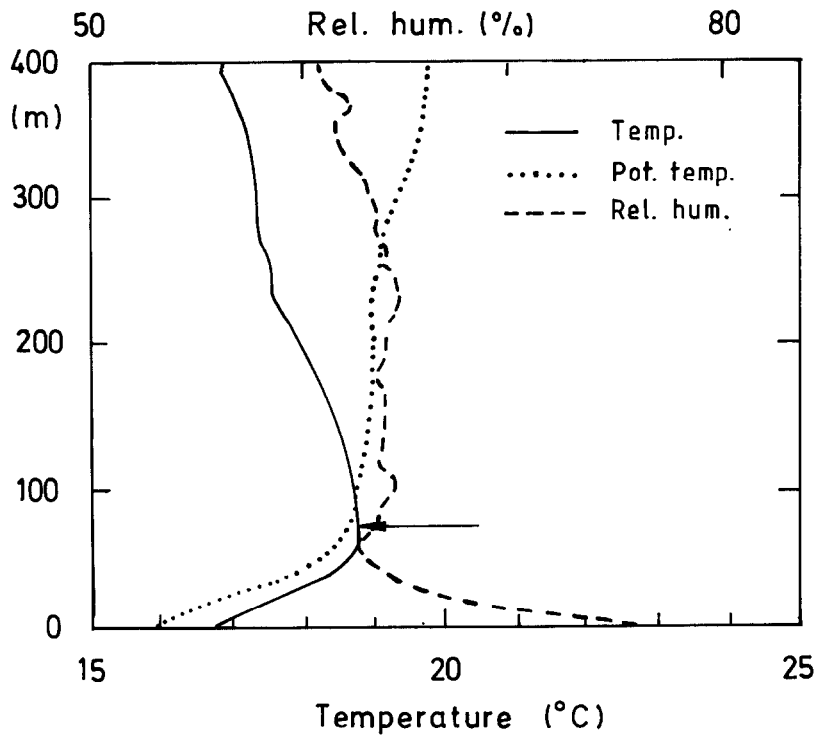

Fig. 4. Minisonde profiles measured at 10.38 CET on 4th of June. The minisonde was launched from a fishing boat at about 12 km from the Swedish coast. The arrows shows the parameterized depth of the stable IBL.

TABLE II

Parameters used for the calculation of the height of the SIBL

Date and time	Fetch	$\Delta\theta s$	Ug	WD	$\bar{U}_r$	H	hcal	hobs
(CET)	(km)	(K)	(m/s)	(deg)	(m/s)	(m)	(m)	(m)
16/5 12.23	14.0	8.0	10.2	169	4.6	11.9	65	63
16/5 13.28	16.1	8.2	9.8	163	4.2	14.2	78	79
16/5 14.43	12.6	8.1	9.7	157	4.2	15.3	84	78
29/5 10.55	13.7	8.5	8.8	98	5.5	13.0	72	76
4/6 10.38	12.0	8.8	16.0	131	7.8	13.7	75	74
5/6 9.29	8.2	7.2	10.8	118	6.6	12.1	67	82

explanation. As was mentioned before, the calculated surface geostrophic winds on that day are considerably lower than the observed ones at 2000 m. This period of disagreement starts between 7.00–10.00 CET and the minisonde was launched at 9.29 CET. Thus, we probably used a value for the surface geostrophic wind that was too low. Using a higher value results in a higher value of the predicted SIBL height. Although additional testing is desirable, the present results clearly indicate that Equation (9) provides very good estimates of the SIBL height.

An interesting consequence of Equation (9) is that when the temperature difference between the land and the sea surface increases, the height of the SIBL decreases. At the same time, the strength of the inversion increases, so the SIBL becomes thinner and more stable.

Mulhearn (1981) suggested an empirical relationship for the height of the SIBL:

$$h = \alpha x (gx\,\Delta\theta_s/\theta u^2)^{-0.47}, \tag{10}$$

where α is a constant equal to 0.0146. Estimates of h obtained from Equation (10) are considerably lower than the values we get in the present analysis and it seems more appropriate to use $\alpha = 0.03$. Garrat and Ryan (1989) found also that, in most cases, Equation (10) with $\alpha = 0.014$ underestimates h and they point out that α is not a constant but depends upon several external parameters.

7. Summary and Conclusions

The Öresund experiment provides a good opportunity to study boundary-layer modification in a coastal area, since simultaneous boundary-layer measurements were obtained over both the sea and the land surface. The case when warm air passes from land over the cooler sea is of special interest, because it has not been studied in any great detail in the past. The underlying hypothesis of the present analysis has been the similarity between the SIBL which develops over the sea, and the horizontally homogeneous, nocturnal boundary layer over the land,

developing during the night. Stull (1983a, b, c) proposed that the time-integrated value of the surface heat flux is more relevant in describing the NBL than the instantaneous value of heat flux. We have found that this applies also for the structure of the SIBL over the water surface.

The variation of the surface heat flux with fetch is parameterized according to Equation (4). This is achieved through suitable nondimensionalization. The velocity scale, defined as $V_s = (fU_g z_0)^{1/2}$, is related to the combined ability of the pressure-gradient force and surface roughness to generate turbulence. The temperature scale is the potential temperature difference between the sea and the land surface. The dimensionless heat flux has a high value immediately after the surface change, and it decreases rapidly in magnitude with increasing distance from the coastline. Farther downwind, the dimensionless heat flux is essentially constant.

The integration of Equation (4) over distance from the shoreline provides the accumulated turbulent cooling within the SIBL. This is used to calculate a heat-flux-history length scale, H, defined by Equation (2).

The potential temperature change at any height, $\Delta\theta(z)$, is described by an exponential profile (Equation 6). Under most circumstances, this implies a negative curvature for the potential temperature profile. In the NBL, a negative curvature in the potential temperature profile is often attributed to dominance of radiational cooling over turbulent cooling. In the present study, we used the potential temperature equation to show that 71% of SIBL cooling is due to turbulence and 29% can be attributed to radiation. Thus, it is proposed that the negative curvature in the potential temperature profile is due to advection.

Finally, following Stull (1983a), we defined the top of the SIBL, h, as that height where the potential temperature decrease is 2% of the surface temperature change. Using Equation (6), we get $h = 5.5H$ which is Equation (9). For the Öresund data set, Equation (9) provides very good estimates for the SIBL height.

Acknowledgements

The Öresund experiment was co-ordinated by NORDFORSK (Nordic co-operative organization for applied research) represented by Mari-Mai Lagus, whose active contribution to the project is very much appreciated. The MIUU participation in the experiment was sponsored by the National Institute of Radiation Protection in Sweden and by the Swedish Natural Science Research Council (NFR contract no G-GU 2684-109). All participants of the Öresund experiment are acknowledged for their excellent work.

References

André, J. C. and Mahrt, L.: 1982, 'The Nocturnal Surface Inversion and Influence of Clear-air Radiative Cooling', *J. Atmos. Sci.* **39**, 864–878.

Brost, R. A. and Wyngaard, J. C.: 1978, 'A Model Study of the Stably Stratified Planetary Boundary Layer', *J. Atmos. Sci.* **39**, 864–878.

Carlson, M. A. and Stull, R. B.: 1986, 'Subsidence in the Nocturnal Boundary Layer', *J. Clim. Appl. Meteorol.* **25**, 1088–1099.

Caughey, S. J., Wyngaard, J. C., and Kaimal, J. C.: 1979, 'Turbulence in the Evolving Stable Boundary Layer', *J. Atmos. Sci.* **36**, 1041–1052.

Doran, J. C. and Gryning, S. E.: 1987, 'Wind and Temperature Structure over a Land-water-land Area', *J. Clim. Appl. Meteorol.* **26**, 973–979.

Garratt, J. R.: 1987, 'The Stably Stratified Internal Boundary Layer for Steady and Diurnally Varying Offshore Flow', *Boundary-Layer Meteorol.* **38**, 369–394.

Garratt, J. R. and Ryan, B. F.: 1989, 'The Structure of the Stably Stratified Internal Boundary Layer in Offshore Flow over the Sea', *Boundary-Layer Meteorol.* **47**, 17–40.

Gryning, S. E.: 1985, 'The Öresund Experiment – A Nordic Mesoscale Dispersion Experiment over a Land-Water-Land Area', *Bull. Am. Meteorol. Soc.* **66**, 1403–1407.

Gryning, S. E. and Joffre, S.: 1987, 'Wind Structure over the Öresund Strait', *The Öresund experiment*, Proc. from Workshop II. Uppsala, October 13–14th, 1987.

Högström, U.: 1988, 'Non-dimensional Wind and Temperature Profiles in the Atmospheric Surface Layer: Reevaluated', *Boundary-Layer Meteorol.* **42**, 55–78.

Hedegaard, K.: 1985, 'Objective Analysis of Pressure Designed for Determination Geostrophic Winds', Weather Service Report No. 4, Danish Meteorological Institute.

Launiainen, J., Grönvall, H. and Vainio, J.: 1987, 'Marine Meteorological Conditions and Air-sea Exchange Characteristics during the Öresund-84 Experiment', *Geophysica* **23**(1).

Melas, D.: 1987, 'Geostrophic Winds in the Öresund Area Determined by Objective Analysis of the Pressure Field', *The Öresund experiment*, Proc. from Workshop II. Uppsala, October 13–14th, 1987.

Mulhearn, P. J.: 1981, 'On the Formation of a Stably Stratified Internal Boundary-Layer by Advevtion of Warm Air over a Cooler Sea', *Boundary-Layer Meteorol.* **21**, 247–254.

Raynor, G. S., SethuRamman, S., and Brown, R. M.: 1979, 'Formation and Characteristics of Coastal Internal Boundary Layers during Onshore Flows', *Boundary-Layer Meteorol.* **16**, 487–514.

Stull, R. B.: 1983a, A Heat-flux-history Length Scale for the Nocturnal Boundary Layer', *Tellus* **35A**, 219–230.

Stull, R. B.: 1983b, 'Integral Scales for the Nocturnal Boundary Layer, Part 1: Empirical Depth Relationships', *J. Climate Appl. Meteorol.* **22**, 673–686.

Stull, R. B.: 1983c, 'Integral Scales for the Nocturnal Boundary Layer, Part 2: Heat Budget, Transport and Energy Implications', *J. Climate Appl. Meteorol.* **22**, 1932–1941.

Stull, R. B.: 1988, *An Introduction to Boundary Layer Meteorology*. pp. 504–506. Atmospheric Sciences Library, Kluwer Academic Publishers, Dordrecht, The Netherlands, 666 pp.